

# **LYVE-1<sup>+</sup> macrophages maintain arterial tone through hyaluronan-mediated regulation of smooth muscle cell collagen**

Hwee Ying Lim<sup>1,12</sup>, Sheau Yng Lim<sup>1,12</sup>, Chek Kun Tan<sup>2</sup>, Chung Hwee Thiam<sup>1</sup>, Chi Ching Goh<sup>3</sup>, Daniel Carbajo<sup>3</sup>, Samantha Hui Shang Chew<sup>1</sup>, Peter See<sup>3</sup>, Svetoslav Chakarov<sup>3</sup>, Xiao Nong Wang<sup>4</sup>, Li Hui Lim<sup>1</sup>, Louise A. Johnson<sup>5</sup>, Chui Yee Fong<sup>6</sup>, Ariff Bongso<sup>6</sup>, Arijit Biswas<sup>6</sup>, Chern Goh<sup>1</sup>, Maximilien Evrard<sup>3</sup>, Kim Pin Yeo<sup>1</sup>, Ranu Basu<sup>7</sup>, , Jun Kit Wang<sup>8</sup>, Yingrou Tan<sup>3</sup>, Rohit Jain<sup>9</sup>, Shweta Tikoo<sup>9</sup>, Cleo Choong<sup>8</sup>, Wolfgang Weninger<sup>9</sup>, Michael Poidinger<sup>3</sup>, Richard E. Stanley<sup>7</sup>, Matthew Collin<sup>4</sup>, Nguan Soon Tan<sup>2,10,11</sup>, Lai Guan Ng<sup>3</sup>, David G. Jackson<sup>5</sup>, Florent Ginhoux<sup>3</sup>, Véronique Angeli<sup>1, 13</sup>

<sup>1</sup>Department of Microbiology & Immunology, Immunology Programme, Life Science Institute, Yong Loo Lin School of Medicine, National University of Singapore, Singapore 117597.

<sup>2</sup>School of Biological Sciences, Nanyang Technological University, Nanyang, Singapore 637551

<sup>3</sup>Singapore Immunology Network, A\*STAR, Singapore 138648.

<sup>4</sup>Institute of Cellular Medicine, Newcastle University, Newcastle, UK NE2 4HH.

<sup>5</sup>MRC Human Immunology Unit, Weatherall Institute of Molecular Medicine, University of Oxford, John Radcliff Hospital, Oxford, UK OX3 9DS

<sup>6</sup>Department of Obstetrics and Gynaecology, Yong Loo Lin School of Medicine, National University Health System, National University of Singapore, Singapore 119074.

<sup>7</sup>Department of Development and Molecular Biology, Albert Einstein College of Medicine, New York 10461, USA

<sup>8</sup>School of Material Science and Engineering, Nanyang Technological University, Singapore 639977

<sup>9</sup>The Centenary Institute, Newtown, New South Wales, 2050 Australia

<sup>10</sup> Institute of Molecular and Cell Biology, A\*STAR, Singapore 138673.

<sup>11</sup> KK Women's and Children Hospital, Singapore 229899.

<sup>12</sup> These authors contributed equally to this work.

<sup>13</sup> Correspondence to:

Véronique Angeli

Department of Microbiology & Immunology, Immunology Programme

National University of Singapore

Centre for Life Sciences, #03-05

28 Medical Drive, Singapore 117456

## Summary

The maintenance of appropriate arterial tone is critically important for normal physiological arterial function. However, the cellular and molecular mechanisms remain poorly defined. Here, we show that in the mouse aorta, resident macrophages prevent arterial stiffness and collagen deposition in the steady state. Using phenotyping, transcriptional profiling and targeted deletion of the *Csf1r* gene, we demonstrate these macrophages which are a feature of blood vessels invested with smooth muscle cells (SMCs) in both mouse and human tissues express the hyaluronan (HA) receptor LYVE-1. Furthermore, we show they possess the unique ability to modulate collagen in SMCs by matrix metalloproteinase MMP-9 dependent proteolysis through engagement of LYVE-1 with the HA pericellular matrix of SMCs. Our study identifies a hitherto unknown homeostatic contribution of arterial LYVE-1<sup>+</sup> macrophages and the first known function of LYVE-1 in leukocytes. Knowledge that LYVE-1<sup>+</sup> macrophages control physiological vascular function reveals new strategies to prevent cardiovascular diseases.

## Introduction

As part of the circulatory system, arteries function to actively transport oxygenated blood nutrients and cells throughout the body in a process that is indispensable for maintaining functional tissue homeostasis. Each artery is composed of three major compartments, namely: the inner intima formed by a single layer of endothelial cells and a fine basement membrane; the media which consists of smooth muscle cell (SMC) layers separated by elastic sheets and the outer adventitial layer that is composed predominantly of connective tissue, mainly collagen fibres and fibroblasts (Wagenseil and Mecham, 2009). While small muscular arteries rely on SMCs to facilitate blood flow, the microstructure of large- and medium-sized elastic arteries including the aorta determines efficient blood flow (Greenwald, 2007). It is the extracellular matrix (ECM) within this microstructure, that is made up of elastin and collagen, which imparts the elastic properties and strength of the aorta, respectively (Kohn et al., 2015).

Changes in the amounts and/or architecture of elastin and collagen in the arterial wall have been shown to affect arterial mechanical function and thus to impede blood flow (Kohn et al., 2015). For example, elastin haploinsufficient and collagenase-resistant mice have been shown to endure arterial mechanical dysfunction and increased vascular wall rigidity (Vafaie et al., 2014; Wagenseil et al., 2005). Furthermore, in humans considerable clinical evidence including genetic studies on patients with Marfan and Williams-Beuren syndrome have clearly implicated arterial ECM remodelling in the pathogenesis of the most common forms of aortic diseases associated with aberrant arterial biomechanics such as aging-induced arterial stiffening, atherosclerosis, aneurysms, and dissections (Tsamis et al., 2013). Remodelling of ECM associated with these pathological conditions often results from the imbalance between production and degradation of collagen and elastin in the arterial wall. Increased ECM synthesis by vascular SMCs and adventitial fibroblasts is mediated by

fibrotic factors such as transforming growth factor- $\beta$  (TGF- $\beta$ ) and prostaglandin F<sub>2</sub> (Border and Noble, 1994; Oga et al., 2009) whereas matrix metalloproteinases (MMPs) and tissue inhibitors of MMPs are involved in the degradation of ECM proteins and its control, respectively (Castro et al., 2011; Wagenseil and Mecham, 2009). While regulators of ECM synthesis and degradation in aortic diseases have been well studied, little is known about effectors and mechanisms that might limit aberrant ECM production and maintain normal aortic tissue elasticity, strength and function in normal physiological conditions.

Tissue resident macrophages are now recognised to fulfill functions beyond those of conventional immune regulation, and to play important roles in support of tissue homeostasis. These latter functions of macrophages are highly dependent on the tissue in which they reside and on changes in their environment to which they respond rapidly (Ginhoux and Jung, 2014; Ginhoux et al., 2015; Kierdorf et al., 2015; Varol et al., 2015). The existence of normal arterial resident macrophage populations defined by their expression of either conventional or more selective lineage markers has been reported previously (Ensan et al., 2016; Galkina et al., 2006; Jongstra-Bilen et al., 2006). Using a gene profiling approach, Ensan et al., have recently reported a unique gene signature for resident arterial macrophages when compared to other tissue macrophages including microglia, alveolar and splenic macrophages during adult murine homeostasis, consistent with the notion that arterial macrophages may be distinctly and functionally different from other tissue macrophages (Ensan et al., 2016). In these models the resident arterial macrophages were replaced by inflammatory infiltrating macrophages upon bacterial infection and returned rapidly to homeostasis when the infection subsided. Although they provided important insights into the origin and maintenance of arterial macrophages these studies failed to explore their physiological function. In fact, whether arterial macrophages regulate arterial homeostasis is still an open question, in part because functional studies to elucidate their role have focused instead on the formation, damage or

repair of blood vessels during developmental and pathogenic processes (Fung and Helisch, 2012; Simons and Eichmann, 2015; Swirski et al., 2016). During ischemic conditions, infiltrating macrophages are thought to promote arteriogenesis (collateral artery formation) by secreting vascular growth factors including vascular endothelial growth factor-A and fibroblast growth factor (Fung and Helisch, 2012; Simons and Eichmann, 2015). The depletion of infiltrating inflammatory macrophage/monocytes was found to ameliorate aneurysm and atherosclerosis progression in mice (Dawson et al., 1999; Moore et al., 2015; Murayama et al., 1999; Randolph, 2014; Wang et al., 2010).

Motivated by the dramatic increase in the current understanding of tissue macrophage homeostatic function, we therefore sought to elucidate whether arterial-resident macrophages contribute to adult vessel integrity. Our current study focussed on murine aorta because this is the largest artery that drains directly from the heart to distribute oxygenated blood through the body and its damage results in life-threatening cardiovascular diseases including arterial stiffness, aneurysms, atherosclerosis and myocardial infarction (Kohn et al., 2015). Our results show for the first time that aortic resident macrophages are essential for the maintenance of arterial vessel homeostasis through the regulation of mural cell collagen production. Furthermore, our studies using phenotyping, gene profiling, targeted deletion of the *Csfr1r* gene and *in vitro* co-culture systems reveal these functions are carried out by a specialised population of arterial macrophages that interact with the extracellular matrix glycosaminoglycan hyaluronan in vascular smooth muscle cells via the lymphatic receptor LYVE-1.

## Results

### Maintenance of arterial macrophages depends on CSF-1/CSF-1R signalling in normal aorta

We first used flow cytometry and fluorescent microscopy to identify macrophages residing in adult murine aorta under steady state conditions. In view of the recent discovery of MerTK and FcγR1 (CD64) as tissue resident macrophages markers (Gautier et al., 2012), we utilized them in our single aortic cell suspension flow cytometry-based analysis. These analyses revealed that MerTK<sup>+</sup>CD64<sup>+</sup> aortic macrophages in adult wild-type (WT) mice were also F4/80<sup>+</sup>CD11b<sup>+</sup> (Figure 1A). Moreover, immunofluorescence analysis of aortic sections showed that CD68<sup>+</sup> macrophages mainly resided within the collagen type I (Col I) rich adventitia in close contact with the medial layer but not within the media and only few macrophages were occasionally detected in the luminal side of the intima (Figure 1B and data not shown). Further examination of the spatial distribution of macrophages within the arterial wall layers by flow cytometry confirmed that macrophage numbers were markedly higher in the adventitia than in the intima/media (Figure 1C), consistent with recent findings in mouse arterial macrophages (Ensan et al., 2016).

To evaluate the contribution of arterial macrophages to vessel homeostasis *in vivo*, we generated a mouse model in which these macrophages are depleted. The macrophage colony stimulating factor (M-CSF) or CSF-1 is critical for the survival, proliferation and differentiation of tissue macrophages through the activation of CSF-1 receptor (CSF-1R) (Hume and MacDonald, 2012). Comparative analyses of *Csf1* and *Csf1r* gene expression in aortas from WT mice revealed that *Csf1* was expressed in both the adventitial and medial layers but at higher levels in adventitia (Figure 1D). In contrast, *Csf1r* was only detected in adventitia where the majority of macrophages reside and the presence of CSF-1R on the surface of aortic macrophages was subsequently confirmed by flow cytometry (Figure 1E). Furthermore, experiments with Fas-induced apoptosis (MaFIA) transgenic mice that express green fluorescent protein (EGFP) under the *Csf1r* promoter (Burnett et al., 2004) revealed a CD68/GFP dual-positive macrophage population in aortic sections (Figure 1F). These

findings indicated that arterial macrophages may also depend on the CSF-1/CSF-1R pathway for their maintenance, and hence we evaluated the effects of CSF1-R inhibition on aortic macrophages in the steady state. As shown in Figures 1G and 1H, treatment for 2 weeks with the selective CSF-1R tyrosine kinase inhibitor, Ki20227 (Kubota et al., 2009; Ohno et al., 2006) indeed resulted in a profound depletion of macrophages in aorta of WT mice when assessed by microscopy and flow cytometry. In sum, these findings identify an essential role for a CSF-1/CSF-1R axis in maintaining aortic macrophage numbers in the steady state and validate the pharmacological inhibition of CSF-1R signalling as an effective means of depleting aortic macrophages *in vivo*.

### **Resident arterial macrophages maintain normal vascular wall structure**

We next evaluated the effect of ablating resident aortic macrophages in the vascular wall. Ki20227 treatment for 14 weeks in WT mice markedly depleted aortic macrophages (Figures 1I and 1J), and the few that remained in the adventitia (Figures 1I and 1J) were no longer in close contact with the medial layer but were instead located predominantly at the outer border of the adventitial layer (Figures 1J and 1K). Notably, monocyte numbers in blood and aortas remained unaffected, showing that Ki20227 treatment does not affect this population (Figures S1A and S1B). Importantly, the depletion of aortic macrophages in Ki20227-treated animals resulted in partial straightening of elastin fibres and significant vessel dilatation (Figures 1J-L). Besides changes in the medial wall, significant adventitial thickening was also observed in Ki20227-treated WT aortas (Figures 1M and 1N). Similar results were obtained in the aortas of MaFIA mice following administration of the drug AP20187 to induce Fas-mediated apoptosis in CSF-1R expressing cells including aortic macrophages (Figures S1C-G). Hence we conclude that the loss of aortic resident macrophages in the steady state is associated with arterial structural changes.

## **Resident arterial macrophages control vascular ECM environment and physiological function**

Since elasticity and strength in the normal aorta is governed by the key ECM proteins collagen and elastin, we hypothesized that arterial macrophages maintain vascular wall integrity by regulating ECM protein expression. Accordingly, we analysed the expression of ECM related genes in aortas from Ki20227-treated WT mice. We found that tropo-elastin (*TropE*), the precursor of elastin was downregulated in the medial layers of Ki20227-treated WT mice whereas pro-collagen type 1 alpha 1 (*Colla1*) was markedly upregulated (Figure 2A). Moreover, the levels of collagen degrading matrix metalloproteinases *Mmp-2* and *Mmp-3* were also decreased. In contrast, other pro-collagen forms, MMP inhibitors (TIMPs) and fibronectin were unaffected in the medial layer of Ki20227-treated WT mice. *TropE* was also down-regulated in the media of MaFIA mouse aortas following macrophage depletion (Figure S1E). ECM changes in the media of Ki20227-treated WT aortas were accompanied by significantly increased expression of *Colla1*, *Col3a1* and decreased expression of *Mmp-9* in the adventitia (Figure 2B). In support of our gene expression analyses, quantification of total collagen protein using Sirius red immunohistochemistry (Lopez-De Leon and Rojkind, 1985), revealed a significantly increased collagen content in Ki20227-treated WT aortas (Figure 2C). Notably, enhanced collagen deposition was also apparent in the medial layer of Ki20227-treated WT aortas (Figure 2D).

Structural modifications of the arterial wall, particularly those affecting the ECM have been reported previously to alter aortic mechanical function and to impede blood flow (Kohn et al., 2015). To determine the consequences of the structural alterations observed in macrophage depleted aortas for the passive mechanical properties of the aortic wall, we performed circumferential tensile assays to assess stress-strain relationship in the vessels. Ki20227-treated WT mice displayed increased aortic wall stiffness compared to the vehicle-treated WT



group, as evidenced by a leftward shift and an increased slope in the stress-strain curve (Figures 2E and 2F), indicating that Ki20227-treated aortas had significantly reduced passive mechanical function. Furthermore, the contractile function of the aortas in Ki20227-treated WT mice was compromised, as shown by a significant reduction in the maximal contractile force of aortic rings generated in response to potassium chloride (Figure 2G). However, these mechanical and functional alterations were not associated with changes in systemic blood pressure (Figures S2A-C). Indeed we could rule out any direct effects of Ki20227 treatment on SMCs in the aortas, as these express neither CSF-1R mRNA nor protein (Figures 1D and 1F).

Next, we investigated the possibility that arterial macrophages might have repopulated the adventitia after the cessation of Ki20227 treatment and hence were able to reverse the defects seen in the arterial wall (Figure S2D). Indeed, we found that arterial macrophage numbers were significantly increased 10 weeks after Ki20227 treatment was terminated (Figure 2H). The repopulated macrophages were located in the adventitia and in the close vicinity of medial SMCs, similar to untreated WT mice (Figure 2I). To evaluate how these cells are replenished, we assessed macrophage repopulation in lethally irradiated CD45.2<sup>+</sup> mice transplanted with congenic CD45.1<sup>+</sup> bone marrow (BM) cells, both before and after Ki20227 treatment (Figure 2J). In agreement with previous findings (Hashimoto et al., 2013), recipient mice achieved almost complete donor chimerism among blood monocytes one month after transplantation. The donor chimerism of aortic monocytes (CD45<sup>+</sup>CD11b<sup>+</sup>Ly6C<sup>+</sup>) remained > 85% both before and after Ki20227 treatment, confirming that they derive from BM cells (Figure 2J). Arterial macrophages were replaced by donor BM cells to the proportion of 64.85% of the population at steady state and 80.48% after depletion, respectively. Notably, these newly replaced-BM derived macrophages were able to reverse arterial remodelling (Figures 2K-N) and function (Figures 2O and P).

Finally, we examined the impact of arterial macrophage depletion on arterial stiffness in atherosclerotic-prone apolipoprotein E deficient (*apoE*<sup>-/-</sup>) mice. Previous studies in such mice had shown that arterial stiffness precedes the formation of atherosclerotic lesions (Gotschy et al., 2013). Consistent with these findings, the descending aortas of 18 week old *apoE*<sup>-/-</sup> mice fed a high-fat diet exhibited increased arterial stiffness as measured by our tensile strength assay and negligible atherosclerosis (Figures S2E-G). Moreover, treatment of *apoE*<sup>-/-</sup> mice with Ki20227 abrogated residual arterial macrophages, and further exacerbated arterial stiffness and collagen deposition in the adventitia with no alterations in systemic blood pressure (Figures 2Q-Y). These data further support the importance of arterial macrophages in preventing arterial stiffness and collagen deposition.

Altogether, these results show that the alterations in vessel structure observed after depletion of arterial macrophages are accompanied by significant changes in aortic biomechanics and infer the maintenance of arterial integrity and function depends on the presence of arterial macrophages under both steady state and pathological conditions.

### **The predominant aortic macrophage population in the steady state express the lymphatic hyaluronan receptor LYVE-1**

Because tissue macrophages are phenotypically and functionally heterogeneous (Varol et al., 2015), we considered the possibility that those responsible for regulating arterial homeostasis might represent a distinct phenotypic subpopulation. In particular we focussed on their expression of LYVE-1, the main hyaluronan receptor in lymphatic vessel endothelium that mediates docking and entry of leukocytes (Banerji et al., 1999; Jackson, 2018; Johnson et al., 2017), but which is also expressed in certain subsets of M2-like tissue macrophages in adipose tissue, eye, skin, brain, aorta and heart (Cho et al., 2007; Ensan et al., 2016; Faraco et al., 2016; Pinto et al., 2012; Schlereth et al., 2014; Xu et al., 2007; Zhang et al., 2010). Consistent with the recent report by Ensan *et al.*, (Ensan et al., 2016), LYVE-1<sup>+</sup> cells were

found to be abundant throughout the entire surface of normal adult mouse aortas when assessed by immunohistochemical staining (Figure 3A). In addition, flow cytometric analysis revealed that MerTK<sup>+</sup>CD64<sup>+</sup>F4/80<sup>+</sup>CD11b<sup>+</sup> aortic macrophages were predominantly LYVE-1<sup>+</sup> (84.49 ± 0.99%) as opposed to LYVE-1<sup>-</sup> (4.94 ± 0.62%) (Figure 3B). LYVE-1<sup>+</sup> macrophages were also positive for the M2 macrophage markers CD163 and CD206 (Bourlier et al., 2008; Canton et al., 2013), (Figure S3A). Further characterization using MHCII showed that the aortas contained equal proportions of MHCII<sup>+</sup> and MHCII<sup>-</sup> LYVE-1<sup>+</sup> macrophages (43.37 ± 1.79% and 37.50 ± 1.5%, respectively; mean ± SEM) (Figure 3B). LYVE-1<sup>+</sup> macrophages resided exclusively within the adventitia and were absent from the media and intima (Figure 3C) whereas both MHCII<sup>-</sup> and MHCII<sup>+</sup> LYVE-1<sup>+</sup> macrophages were often found spatially associated with the medial layer (Figures 3D and 3E). In contrast, LYVE-1<sup>-</sup> macrophages were rarely observed in the aortic adventitia at steady state (Figure 3D). Further examination of the spatial distribution of macrophages within the arterial layers by flow cytometry confirmed that LYVE-1<sup>+</sup> macrophage numbers were markedly higher in the adventitia than in the intima/media (Figure 3F).

LYVE-1 expression in these arterial macrophages is apparently not required for their development and persistence in the adult aorta, at least under normal condition since CD68<sup>+</sup> macrophages remained abundant in the adventitial layer of *Lyve-1*<sup>-/-</sup> mice, in close contact with medial SMCs and expressed CD163 (Figures S3B and S3C). Moreover, in line with the recent report by Ensan *et al.*, we detected CX3CR1<sup>+</sup> macrophages in aortas of *Cx3cr1*<sup>gfp/+</sup> mice (Figures S3D and S3E) (Ensan et al., 2016). However, only a fraction of LYVE-1<sup>+</sup> macrophages expressed CX3CR1 (Figures S3D and S3E). Analysis of MaFIA mouse aortic sections confirmed that LYVE-1<sup>+</sup> macrophages expressed CSF-1R (Figure 3G) and flow cytometric analysis revealed that CSF-1R expression was more abundant on the surface of aortic LYVE-1<sup>+</sup> macrophages than LYVE-1<sup>-</sup> macrophages (Figure 3H). Consistent with the

role of CSF-1/CSF-1R signalling in maintenance of arterial MerTK<sup>+</sup>CD64<sup>+</sup> macrophage survival (Figures 1G and 1H), treatment for 2 weeks with Ki20227 drug resulted in a profound depletion of LYVE-1<sup>+</sup> macrophages in aortas of WT mice (Figures 3I and 3J). Together, these findings raise the possibility that depletion of these cells, which represent the predominant population of macrophages residing in mouse aortas, may contribute to the arterial stiffness and collagen deposition observed after Ki20227 treatment.

**LYVE-1<sup>+</sup> macrophages are universally associated with blood vessels invested by smooth muscle cells in both mouse and human tissues**

We next assessed whether the LYVE-1<sup>+</sup> macrophage population observed in the aorta also lines the blood vasculature of other tissue/organs. To investigate the 3D spatial distribution of LYVE-1<sup>+</sup> cells in mouse skin, we utilized multi-photon microscopy to visualise ear skin whole mount preparations. LYVE-1<sup>+</sup> cells first appeared below the uppermost part of the dermis (~38  $\mu$ m) and persisted throughout the deeper dermis (below 80  $\mu$ m; Figure 4A). We also made the unexpected observation that some but not all LYVE-1<sup>+</sup> cells aligned with each other to form “train track” structures (Figure 4A and Video S1) suggesting that such cells are associated with vessels. A subset of LYVE-1<sup>+</sup> cells was indeed arranged along large CD31<sup>+</sup> vessels in the deeper dermis (below ~38  $\mu$ m) whereas no LYVE-1<sup>+</sup> cells were associated with smaller CD31<sup>+</sup> vessels or initial lymphatic in the uppermost dermis (0-34  $\mu$ m; Figure 4A and Video S1). In the skin, the blood vasculature mainly consists of arterioles and venules which are surrounded by SMCs expressing smooth muscle actin (SMA) and capillaries that are covered by SMA<sup>-</sup> pericytes (Gerhardt and Betsholtz, 2003). Triple staining for SMA, LYVE-1 and CD31 revealed that LYVE-1<sup>+</sup> cells lined vessels invested with SMA<sup>+</sup> SMCs but not the smaller SMA<sup>-</sup> capillaries (Figures 4B, 4C and Video S2). Co-staining of whole mount tissues with CD68, CD206 and CSF-1R also confirmed that LYVE-1<sup>+</sup> macrophages underlined perivascular SMCs in skin (Figures 4D and S4A).

We also investigated the presence of such LYVE-1<sup>+</sup> macrophages in the central nervous system. Consistent with recent observations in the mouse brain (Faraco et al., 2016; Zeisel et al., 2015), LYVE-1<sup>+</sup> macrophages were associated with pial, penetrating parenchymal and meningeal SMC<sup>+</sup> vessels but not SMC<sup>-</sup> vessels (Figures 4E, 4F, S4C and S4D). LYVE-1<sup>+</sup> macrophages also lined SMA<sup>+</sup> blood vessels in other vascularized mouse tissues including adipose tissues and tracheae (Figures 4G and S4B). Finally, these perivascular LYVE-1<sup>+</sup> macrophages were not restricted to mouse vessels but were also found on human SMA<sup>+</sup> vasculature in the dermis of abdominal skin (Figures 4H and S4E) and in umbilical cord (Figure 4I). Together, these data reveal the exclusive distribution of LYVE-1<sup>+</sup> macrophages in the adventitia of SMA<sup>+</sup> large blood vessels, a feature that may well explain why the aorta, which is rich in SMCs, predominantly consisted of LYVE-1<sup>+</sup> macrophages. These results also provide preliminary evidence that this subset of perivascular LYVE-1<sup>+</sup> macrophages is conserved across different organs/tissues and species.

### **LYVE-1<sup>+</sup> and LYVE-1<sup>-</sup> aortic macrophages are functionally distinct**

To gain insight into the functions of arterial LYVE-1<sup>+</sup> and LYVE-1<sup>-</sup> macrophages, we performed gene expression profiling using RNA sequencing. Transcriptional profiling revealed 288 genes that were significantly differentially expressed between aortic LYVE-1<sup>+</sup> and LYVE-1<sup>-</sup> macrophages. Among them, LYVE-1<sup>+</sup> macrophages displayed 125 positively regulated and 163 negatively regulated genes relative to LYVE-1<sup>-</sup> macrophages (Figure 5A and Table S1). We performed functional enrichment analyses on the two groups of differentially expressed genes to account for the biological processes in which they are involved, based on Gene Ontology annotation. We found that genes upregulated in LYVE-1<sup>-</sup> macrophages were enriched for terms related to immune responses and antigen processing whereas genes that were more abundant in LYVE-1<sup>+</sup> macrophages were enriched for terms related to a broad range of homeostatic processes including metabolism, angiogenesis, elastin

catabolism, cardiac muscle growth and communication (Figures 5B, 5C and Table S2). These data reveals that LYVE-1<sup>+</sup> and LYVE-1<sup>-</sup> macrophages are functionally distinct with LYVE-1<sup>+</sup> macrophages having more of an involvement with tissue homeostasis .

We therefore hypothesized that LYVE-1<sup>+</sup> macrophages, which represent the predominant population of resident arterial macrophages, are the homeostatic regulators of arterial function. To address this hypothesis, *Lyve-1<sup>Cre</sup>* mice (Pham et al., 2010) were crossed with *Csf1r* floxed mice (*Csf1r<sup>flox/flox</sup>*) (Li et al., 2006) to generate *Lyve-1<sup>wt/Cre</sup>;Csf1r<sup>flox/flox</sup>* mice, in which *Csf1r* was specifically depleted in all LYVE-1 expressing cells. Since LYVE-1<sup>+</sup> macrophages depend on the CSF-1/CSF-1R pathway for development, LYVE-1<sup>+</sup> macrophages are depleted in *Lyve-1<sup>wt/Cre</sup>;Csf1r<sup>flox/flox</sup>* mice. Indeed, such mice showed depletion of LYVE-1<sup>+</sup> macrophages in the aortas regardless of their MHC class II expression whereas LYVE-1<sup>-</sup> macrophages, blood and aortic monocytes were not affected (Figures 5D-I). Using this mouse model lacking specifically LYVE-1<sup>+</sup> macrophages, we then determined the consequences of their absence on arterial stiffness and ECM remodelling. Luminal diameter (Figure 5K), adventitial area (Figures 5J and 5L) and collagen deposition (Figures 5M and 5N) were increased in *Lyve-1<sup>wt/Cre</sup>;Csf1r<sup>flox/flox</sup>* mice compared to control *Csf1r<sup>flox/flox</sup>* mice. These structural modifications were accompanied by an increase in aortic wall stiffness without any changes in maximal contractile force (Figures 5O and 5P). Similar to WT mice treated with Ki20227, blood pressure was not altered in *Lyve-1<sup>wt/Cre</sup>;Csf1r<sup>flox/flox</sup>* (Figures 5Q-S). Next, we investigated whether the absence of LYVE-1<sup>+</sup> macrophages leads to similar collagen deposition in tissues other than aorta, specifically intestine and oesophagus of the gastrointestinal tract. Intestinal macrophages were predominantly LYVE-1<sup>-</sup> although occasional LYVE-1<sup>+</sup> macrophages were seen in the submucosal layer (data not shown). In contrast, LYVE-1<sup>+</sup> macrophages were abundant in murine oesophagus and were located mostly in the muscularis mucosa where SMCs reside and in the connective tissue of the

submucosa (Figure S5A). Similar to aortic macrophages, oesophageal macrophages were depleted in  $Lyve-1^{wt/Cre};Csf1^{flox/flox}$  mice (Figure S5A). Moreover, the absence of oesophageal LYVE-1<sup>+</sup> macrophages in these mice resulted in accumulation of collagen in the muscularis mucosa and submucosa (Figures S5B-D).

Altogether, these results highlight the unique function of LYVE-1<sup>+</sup> macrophages in preventing arterial stiffness and collagen deposition. Furthermore, they indicate that LYVE-1<sup>+</sup> macrophage association with SMCs is not restricted to vascular SMCs and that the control of collagen deposition by LYVE-1<sup>+</sup> macrophages is likely a general phenomenon, and not one specific to the aorta.

**Engagement of LYVE-1<sup>+</sup> macrophages with HA on SMCs and MMP-9-dependent proteolysis are required for the regulation of arterial collagen production.**

*Ex vivo* analysis of the phagocytic capacity of aortic LYVE-1<sup>+</sup> and LYVE-1<sup>-</sup> macrophages revealed that both macrophage subsets displayed similar phagocytic properties (Figure S6A). Moreover, LYVE-1<sup>+</sup> macrophages lining blood vessels in skin were also phagocytic based on their ability to ingest fluorescent dextran following intradermal injection (Figure S6B). These data indicate that LYVE-1<sup>+</sup> macrophages contribute to arterial homeostatic function via a tissue-process other than phagocytosis. Since vascular integrity and contractile function are regulated by ECM proteins produced largely by SMCs (Wagenseil and Mecham, 2009), we reasoned that LYVE-1<sup>+</sup> macrophages might exert their effects by modulating SMC function. We first examined the effect of LYVE-1<sup>+</sup> macrophages on the production of collagen by primary cultured murine aortic SMCs *in vitro* (Figure S7A). Because of the limited recoveries of LYVE-1<sup>+</sup> and LYVE-1<sup>-</sup> macrophages from aortas after cell sorting, we instead used macrophages sorted from mouse adipose tissues for these *in vitro* co-culture systems. Importantly, LYVE-1<sup>+</sup> macrophages were the predominant resident macrophage population

in adipose tissue, exhibited higher levels of CSF-1R compared to LYVE-1<sup>-</sup> macrophages and expressed genes enriched for terms related to key homeostatic processes, similar to their aortic LYVE-1<sup>+</sup> macrophage counterparts (Figures S7B-F and Tables S3-4). While addition of LYVE-1<sup>-</sup> macrophages to cultured SMCs exerted no effect on the levels of Collagen type I (Col I), the most abundant ECM protein in aortic wall (Murata K, 1986), addition of such LYVE-1<sup>+</sup> macrophages induced a significant reduction (Figures 6A and 6B). Together, these data show that LYVE-1<sup>+</sup> macrophages have a unique ability to modulate the collagen content in vascular SMCs.

We next investigated the mechanisms by which LYVE-1<sup>+</sup> macrophages regulate SMC collagen *in vitro*. The reduced production of Col I protein in SMCs observed in the presence of LYVE-1<sup>+</sup> macrophages likely resulted from protein degradation rather than transcriptional regulation, since we did not observe marked differences in *colla1* gene expression (Figure S7G). MMPs contribute to vascular ECM homeostasis through the degradation of ECM proteins and also prevent overload of ECM components (Castro et al., 2011). The depletion of MMP-9 in rodents is known to aggravate arterial stiffness and increases vascular collagen content (Flamant et al., 2007). Indeed, macrophages have been shown to express MMP-9 (Yabluchanskiy et al., 2013). In our study, aortic adventitial *Mmp-9* mRNA expression was significantly decreased following macrophage depletion (Figure 2B) and higher levels of *Mmp-9* mRNA were detected in LYVE-1<sup>+</sup> macrophages compared to LYVE-1<sup>-</sup> macrophages sorted from adult WT adipose tissues (Figure 6C). Immunofluorescence analysis of WT aortic sections revealed MMP-9 expression in adventitial LYVE-1<sup>+</sup> macrophages and in the intima layers, with minimal amounts being detected in the medial SMCs (Figure 6D). Next, we assayed for MMP-9 activity in aortic sections by gelatin-based *in situ* zymography. Using this method, we detected proteolytic activity in the periadventitial fat, as well as the adventitial and medial layers in WT and control *Csf1r*<sup>flox/flox</sup> mice. In contrast, this activity



was markedly reduced in the periadventitial fat and adventitial layers of Ki20227-treated WT mice and *Lyve-1*<sup>wt/Cre</sup>;*Csf1r*<sup>flx/flx</sup> mice (Figure 6E) whereas it remained unaltered in the media of these mice. These findings suggested that LYVE-1<sup>+</sup> macrophages might utilise MMP-9 to degrade SMC collagen and thus we initially evaluated the effects of adding a selective MMP-9 inhibitor in our LYVE-1<sup>+</sup> macrophage / SMC *in vitro* co-culture system. Consistent with this explanation, addition of the MMP-9 inhibitor to cultured SMCs alone had no effect on Col I levels which remained unchanged compared to untreated controls (Figures 6F and G). In contrast, when added to SMCs co-cultured with LYVE-1<sup>+</sup> macrophages, the reduction in Col I levels exerted by the latter was partly reversed (Figures 6F and G), indicating MMP-9 derived from these LYVE-1<sup>+</sup> macrophages was responsible for the Col I degradation. This was indeed confirmed when LYVE-1<sup>+</sup> macrophages sorted from MMP-9 deficient mice were cultured with SMCs, since these had no such effect on Col I (Figures 6H and 6I). Hence we conclude that LYVE-1<sup>+</sup> macrophages regulate collagen content in vascular SMCs, to a significant degree via MMP-9 dependent proteolysis. Interestingly however, the collagen degradative activity of LYVE-1<sup>+</sup> macrophages was not recapitulated when purified pro- or active forms of MMP-9 were added instead to cultured SMCs (Figure S8A), suggesting that such macrophages played an additional potentiating role in the process.

With regard to this possibility, recent reports have shown that MMP-9 can act pericellularly through its interaction with cell surface components (Murphy and Nagase, 2011). Thus, we hypothesized that MMP-9 may be sequestered on the surface of LYVE-1<sup>+</sup> macrophages and that a direct macrophage:SMC cell:cell interaction may be required to focus its proteolytic activity on Col I. To test this hypothesis, we used a transwell system to separate the two cell types. Indeed, when LYVE-1<sup>+</sup> macrophages were prevented from making physical contact with vascular SMCs in this way, they lost the capacity to degrade

SMC collagen (Figure 6J). We then sought to identify the components required for this critical LYVE-1<sup>+</sup> macrophage / SMC interaction. Since MMP-9 has been shown to localize pericellularly through its binding to  $\beta$ -integrin and CD44 (Redondo-Munoz et al., 2008; Yu and Stamenkovic, 2000), we evaluated the involvement of both these receptors using specific blocking mAbs. Neither blocking integrin beta-1 (ITGB1) nor CD44 affected the capacity of LYVE-1<sup>+</sup> macrophages to alter collagen levels in SMCs (Figure S8B). Since CD44 expression was comparable in LYVE-1<sup>+</sup> and LYVE-1<sup>-</sup> macrophages (Figure S8C) and LYVE-1, in common with CD44 is a receptor for hyaluronan (HA), we went on to block LYVE-1 with two specific mAbs, 2125 and C1/8 that specifically target the LYVE-1 HA binding site (Banerji et al., 2010; Johnson et al., 2017). As shown in Figure 6K, degradation of collagen in SMCs by LYVE-1<sup>+</sup> macrophages was abrogated in the presence of either of these mAbs. These results suggested either that LYVE-1 sequesters MMP-9 via its HA-binding site, or that the receptor mediates the critical macrophage/SMC interaction required for MMP-9 dependent collagen degradation, by engaging with HA in the SMC pericellular matrix (Figure 6K). Finally to distinguish between these two different possibilities, we specifically depleted the pericellular HA on SMCs by hyaluronidase treatment (Figure S8D). Such depletion completely abrogated the collagenolytic effect of LYVE-1<sup>+</sup> macrophages (Figure 6L), confirming these cells exert their critical regulation of matrix homeostasis and vessel mechanics through HA-dependent SMC adhesion.

## **Discussion**

Despite initial studies reporting the occurrence of resident arterial macrophages under steady state conditions (Ensan et al., 2016; Faraco et al., 2016; Galkina et al., 2006; Jongstra-Bilen et al., 2006) and their functional involvement during inflammation and vascular diseases

(Fung and Helisch, 2012; Simons and Eichmann, 2015; Swirski et al., 2016), ours is the first study to show that these cells sustain large blood vessel functional homeostasis, in part by modulating the ECM environment. Moreover our results show that tissue-resident macrophages, rather than acting as passive bystanders, may well have additional functions beyond the classically described roles of phagocytosis, inflammation, wound-healing and fibrosis. Our work also further illustrates the specialized physiological function of resident macrophages in the tissue in which they reside (Ginhoux and Jung, 2014; Ginhoux et al., 2015; Kierdorf et al., 2015; Varol et al., 2015).

The ECM architecture of large arteries is an important feature designed to withstand the large blood volume pumped from the heart with little or no change in blood pressure (Kohn et al., 2015). The abnormal remodelling of aortic ECM has major detrimental consequences including contractile dysfunction, aberrant mechanosensing and compromised arterial integrity collectively referred to as arterial stiffness, that eventually diminish the capacity of vessels to accommodate cardiac load (Kohn et al., 2015). In recent years, several studies have reported the prognostic value of arterial stiffness in patient- and general population-based cohorts as an independent predictor of cardiovascular events, cardiovascular morbidity and all-cause mortality (Blacher et al., 1999; Mitchell et al., 2010; Palombo and Kozakova, 2016; Vlachopoulos et al., 2010). In line with these epidemiological findings, animal models of arterial stiffness associated with ECM remodelling have revealed fatal cardiovascular diseases and complications such as ischemia, aneurysms and atherosclerosis (Kothapalli et al., 2012; Lacolley et al., 2014). Therefore, understanding the mechanisms regulating vascular ECM amount and production is crucial for developing therapies to prevent or limit arterial stiffness. We show here that depletion of arterial macrophages in healthy aorta led to reduced contractile function and increased aortic stiffness and collagen production. These defects were reversed by functional replenishment of arterial macrophages that derived from

BM cells. Moreover, arterial stiffness associated with atherosclerosis was exacerbated when arterial macrophages were depleted. In both models, arterial stiffness was not associated with any changes in blood pressure. This is consistent with data showing that blood pressure is not modified despite marked arterial remodelling and/or arterial stiffness as observed in the well-established angiotensin II-induced aneurysm apoE<sup>-/-</sup> mouse model (Daugherty et al., 2000) and in aged wild-type mice (Francia et al., 2004). Our data reveal arterial macrophages as novel regulators of vascular homeostatic function that have potentially beneficial effects on arterial stiffness and cardiovascular diseases through their ability to regulate ECM production. He and co-workers have demonstrated the importance of perivascular macrophages residing in SMC<sup>+</sup> small blood vessels, namely capillaries, for the control of vascular permeability (He et al., 2016). Therefore, our study along with this latter report support the notion that under physiological conditions, the blood vasculature is actively maintained (Murakami and Simons, 2009) and highlights the functional diversity and specialization of perivascular macrophages, depending on the type of vessels in which they reside.

Functional diversity also seems to be apparent within the same type of vessel, likely reflecting a high degree of macrophage heterogeneity. Indeed, in our study which has focussed on the aorta, assessment of LYVE-1 expression in the steady state by flow cytometry and immunostaining revealed that the aorta contains two distinct populations of macrophages, namely: LYVE-1<sup>-</sup> and LYVE-1<sup>+</sup> macrophages, of which the latter are the most numerous residents. Additional heterogeneity among aortic macrophages was further unveiled by including the functional marker MHCII. The differential expression of MHCII on the surface of LYVE-1<sup>+</sup> macrophages further sub-divided this population into LYVE-1<sup>+</sup>MHCII<sup>+</sup> and LYVE-1<sup>+</sup>MHCII<sup>-</sup>, whereas all LYVE-1<sup>-</sup> macrophages were MHCII<sup>+</sup>. Furthermore, we showed that some but not all LYVE-1<sup>+</sup> macrophages express CX3CR1.

Similar subpopulations of tissue-resident macrophages based on MHCII and CX3CR1 marker expression have been described for dermal, cardiac and intestinal lamina propria resident macrophages (Bain et al., 2013; Epelman et al., 2014; Tamoutounour et al., 2013; Tamoutounour et al., 2012). Hence, there is more phenotypic heterogeneity among arterial macrophages than previously appreciated (Ensan et al., 2016).

Though these aortic LYVE-1<sup>-</sup> and LYVE-1<sup>+</sup> macrophage subpopulations exhibited similar phagocytic properties and relied on CSF-1/CSF-1R pathway for maintenance, they appear to have distinct functions within the vessel wall. Supporting evidence includes our *in vivo* data showing that specific depletion of LYVE-1<sup>+</sup> macrophages in *Lyve-1<sup>wt/Cre</sup>;Csf1r<sup>flox/flox</sup>* mice results in increased arterial stiffness and collagen deposition, our *in vitro* findings showing that LYVE-1<sup>+</sup> but not LYVE-1<sup>-</sup> macrophages can act on SMCs to limit collagen expression and our transcriptome profiling of these two subsets of macrophages identifying genes enriched in various local homeostatic processes and immune response in LYVE-1<sup>+</sup> and LYVE-1<sup>-</sup> macrophages, respectively. Therefore, our results reveal LYVE-1<sup>+</sup> macrophages as the key macrophage subset that maintains arterial wall homeostasis by modulating collagen levels in SMCs. However, we do not rule out the possibility of LYVE-1<sup>+</sup> macrophages interacting with other cell types in the aorta, particularly adventitial fibroblasts that have been reported to modulate ECM production upon injury (Majesky et al., 2011). These functional findings may also explain why LYVE-1<sup>+</sup> macrophages exclusively associate with SMC invested blood vessels but not capillaries which exhibit pericytes but not SMCs. It is plausible that LYVE-1<sup>+</sup> macrophages participate similarly in regulating the blood vasculature of other tissues/organs than the aorta since we found them in skin, trachea, adipose tissue, intestine and brain. They may also regulate collagen deposition by non-vascular SMCs as suggested by our observation in oesophagus. Finally, our confirmation that LYVE-1<sup>+</sup> macrophages are also associated with SMC<sup>+</sup> blood vessels in human skin and umbilical cord

is an indication of the relevance of our observations in mice to the situation in human physiology.

Our preliminary studies on the mechanisms by which LYVE-1<sup>+</sup> macrophages regulate collagen levels in SMCs identified MMP-9 as a potential mediator. Although overexpression of MMP-9 has been considered detrimental to various cardiovascular complications including vascular calcification, myocardial infarction and atherosclerosis (Yabluchanskiy et al., 2013), its beneficial function has been highlighted in early hypertensive arterial stiffness and vein grafting since MMP-9 null mice developed increased vascular stiffness and enhanced collagen deposition (Flamant et al., 2007; Thomas and Newby, 2010), in line with our current study. We do acknowledge that our current study on MMP-9 was limited to *in vitro* investigations and it remains to be determined if the lack of MMP-9 specifically in LYVE-1<sup>+</sup> macrophages alone might impact vascular function. The negative effect of LYVE-1<sup>+</sup> macrophages on SMC collagen is unlikely due to increased SMC differentiation because addition of LYVE-1<sup>+</sup> macrophages to SMCs did not affect the expression of contractile genes in SMCs or their proliferation (data not shown) (Owens et al., 2004; Rensen et al., 2007). Our data also demonstrate that modulation of collagen levels by LYVE-1<sup>+</sup> macrophages is dependent on engagement of the receptor with HA on SMCs. Recent work has demonstrated that dendritic cell (DC) trafficking in lymph involves the engagement of LYVE-1 in lymphatic endothelium with HA present in the DC surface glycocalyx (Johnson et al., 2017). Unlike other members of the Link HA receptor superfamily that includes CD44 and Stabilin-2, LYVE-1 is unique in functioning as a disulphide-linked homodimer (Banerji et al., 2016) whose unusual properties allow the receptor to distinguish higher-order HA configurations on cell surfaces from ambient HA in the interstitial matrix through differences in binding avidity (Jackson, 2018). Such properties may well explain how LYVE-1 engages selectively with the SMC HA pericellular matrix to modulate SMC collagen (Banerji et al., 2010; Jackson, 2018)

Clearly resolution of this latter issue will require further investigations that are beyond the scope of our present study.

In sum, our work addresses previously unanswered questions regarding the homeostatic contribution of arterial macrophages to blood vessels in the adult, and their potential ability to regulate vascular tone in the steady state. These novel biological insights should aid in the development or improvement of existing therapies for the treatment of arterial diseases. This study also reveals the phenotypic and functional heterogeneity of macrophages residing within arteries and in the LYVE-1<sup>+</sup> macrophage subset in particular, as the mediator of this homeostatic function.

## **Experimental Procedures**

### **Mice and human samples**

All animals were maintained in specific pathogen-free animal facility and were handled in accordance to protocols approved by the institutional animal care and use committees (IACUC) of the National University of Singapore and Singapore Immunology Network. A detailed list of various mouse strains and treatment is provided in Supplementary Methods. Human skin was obtained from healthy subject under a Tang Tock Seng Hospital institutional review board-approved protocol after informed consent in accordance with the Declaration of Helsinki. Human umbilical cords were obtained after full term delivery of healthy infants from the National University Hospital and their use in this project was approved by the Ministry of Health Institutional Domain Specific Review Board (DSRB), Singapore after written informed patient consent. No samples or animals were excluded from any analyses. For animal studies, samples were not randomized to experimental groups and animal

numbers were empirically determined to optimize numbers necessary based on our previous studies or pilot experiments. All analyses were performed unblinded except for quantification of numbers of LYVE-1<sup>+</sup> macrophages and assessment of arterial wall remodeling in mice.

### **Tissue processing, flow cytometry and sorting**

Single-cell suspensions from mouse blood, aorta and adipose tissues were generated, stained, analysed and purified as described previously (Cho et al., 2007). Detail information on the experimental procedures can be found in Supplementary Methods.

### **Immunohistochemistry**

Immunofluorescence staining for skin and aorta tissues were performed as previously described (Lim et al., 2013). See Extended Experimental Procedures for more details including reagents, antibodies and microscopes.

### **Vascular smooth muscle cell culture**

Primary mouse vascular smooth muscle cells were isolated from thoracic aorta of 6-8 week old male C57/BL6 mice as previously described (Kothapalli et al., 2012). Details are provided in the Extended Experimental Procedures.

### **Circumference tensile and contractility tests**

Aortic rings from vehicle and Ki20227-treated mice were subjected to tensile and contractility tests accordingly to previously described protocols (Tan et al., 2013). Detailed information on the experimental procedures can be found in Supplementary Methods.

### **RNA sequencing**

Refer to Extended Experimental Procedures for more information.



## **Real time PCR**

Real-time PCR was performed using commercially available kits with some modifications described in Extended Experimental Procedures.

## **Statistical analysis**

Statistical analysis was performed with Graphpad Prism version 5.0 (GraphPad Software). Data were presented as mean  $\pm$  SEM and were analyzed by nonparametric Mann-Whitney U and Kruskal-Wallis tests for comparison between 2 groups and multiple groups ( $\geq 3$ ), respectively for *in vivo* work. For *in vitro* studies, one-way ANOVA was used for multiple group comparisons. A *p* value of less than 0.05 was considered to be statistically significant.

## **Acknowledgements**

We thank Prof Kent Shortman for critical discussion, Mr Y.L Chua for technical assistance and Mr. T. Guohui and Dr. P.E Hutchinson from Flow Cytometry Lab and Dr E. Koh, from Advanced Imaging core facility (Life Science Institute, Immunology programme, National University of Singapore) for sharing their expertise. This work was supported by National Medical Research Council and National Research Foundation grants to Véronique Angeli and UK Medical research Council funding to David Jackson.

## References

- Bain, C.C., Scott, C.L., Uronen-Hansson, H., Gudjonsson, S., Jansson, O., Grip, O., Guillems, M., Malissen, B., Agace, W.W., and Mowat, A.M. (2013). Resident and pro-inflammatory macrophages in the colon represent alternative context-dependent fates of the same Ly6Chi monocyte precursors. *Mucosal immunology* 6, 498-510.
- Banerji, S., Hide, B.R., James, J.R., Noble, M.E., and Jackson, D.G. (2010). Distinctive properties of the hyaluronan-binding domain in the lymphatic endothelial receptor Lyve-1 and their implications for receptor function. *J Biol Chem* 285, 10724-10735.
- Banerji, S., Lawrance, W., Metcalfe, C., Briggs, D.C., Yamauchi, A., Dushek, O., van der Merwe, P.A., Day, A.J., and Jackson, D.G. (2016). Homodimerization of the Lymph Vessel Endothelial Receptor LYVE-1 through a Redox-labile Disulfide Is Critical for Hyaluronan Binding in Lymphatic Endothelium. *J Biol Chem* 291, 25004-25018.
- Banerji, S., Ni, J., Wang, S.X., Clasper, S., Su, J., Tammi, R., Jones, M., and Jackson, D.G. (1999). LYVE-1, a new homologue of the CD44 glycoprotein, is a lymph-specific receptor for hyaluronan. *The Journal of cell biology* 144, 789-801.
- Blacher, J., Guerin, A.P., Pannier, B., Marchais, S.J., Safar, M.E., and London, G.M. (1999). Impact of aortic stiffness on survival in end-stage renal disease. *Circulation* 99, 2434-2439.
- Border, W.A., and Noble, N.A. (1994). Transforming growth factor beta in tissue fibrosis. *N Engl J Med* 331, 1286-1292.
- Bourlier, V., Zakaroff-Girard, A., Miranville, A., De Barros, S., Maumus, M., Sengenès, C., Galitzky, J., Lafontan, M., Karpe, F., Frayn, K.N., *et al.* (2008). Remodeling phenotype of human subcutaneous adipose tissue macrophages. *Circulation* 117, 806-815.
- Burnett, S.H., Kershen, E.J., Zhang, J., Zeng, L., Straley, S.C., Kaplan, A.M., and Cohen, D.A. (2004). Conditional macrophage ablation in transgenic mice expressing a Fas-based suicide gene. *J Leukoc Biol* 75, 612-623.
- Canton, J., Neculai, D., and Grinstein, S. (2013). Scavenger receptors in homeostasis and immunity. *Nat Rev Immunol* 13, 621-634.
- Castro, M.M., Tanus-Santos, J.E., and Gerlach, R.F. (2011). Matrix metalloproteinases: targets for doxycycline to prevent the vascular alterations of hypertension. *Pharmacol Res* 64, 567-572.
- Cho, C.H., Koh, Y.J., Han, J., Sung, H.K., Jong Lee, H., Morisada, T., Schwendener, R.A., Brekken, R.A., Kang, G., Oike, Y., *et al.* (2007). Angiogenic role of LYVE-1-positive macrophages in adipose tissue. *Circ Res* 100, e47-57.
- Daugherty, A., Manning, M.W., and Cassis, L.A. (2000). Angiotensin II promotes atherosclerotic lesions and aneurysms in apolipoprotein E-deficient mice. *J Clin Invest* 105, 1605-1612.
- Dawson, T., Kuziel, W., Isahar, T., and Maeda, N. (1999). Absence of CC chemokine receptor-2 reduces atherosclerosis in apolipoprotein E-deficient mice. *Atherosclerosis* 143, 205-211.
- Ensan, S., Li, A., Besla, R., Degousee, N., Cosme, J., Roufaiel, M., Shikatani, E.A., El-Maklizi, M., Williams, J.W., Robins, L., *et al.* (2016). Self-renewing resident arterial macrophages arise from embryonic CX3CR1(+) precursors and circulating monocytes immediately after birth. *Nat Immunol* 17, 159-168.
- Epelman, S., Lavine, K.J., Beaudin, A.E., Sojka, D.K., Carrero, J.A., Calderon, B., Brijia, T., Gautier, E.L., Ivanov, S., Satpathy, A.T., *et al.* (2014). Embryonic and adult-derived resident cardiac macrophages are maintained through distinct mechanisms at steady state and during inflammation. *Immunity* 40, 91-104.

Faraco, G., Sugiyama, Y., Lane, D., Garcia-Bonilla, L., Chang, H., Santisteban, M.M., Racchumi, G., Murphy, M., Van Rooijen, N., Anrather, J., *et al.* (2016). Perivascular macrophages mediate the neurovascular and cognitive dysfunction associated with hypertension. *J Clin Invest* 126, 4674-4689.

Flamant, M., Placier, S., Dubroca, C., Esposito, B., Lopes, I., Chatziantoniou, C., Tedgui, A., Dussault, J.C., and Lehoux, S. (2007). Role of matrix metalloproteinases in early hypertensive vascular remodeling. *Hypertension* 50, 212-218.

Francia, P., delli Gatti, C., Bachschmid, M., Martin-Padura, I., Savoia, C., Migliaccio, E., Pelicci, P.G., Schiavoni, M., Luscher, T.F., Volpe, M., *et al.* (2004). Deletion of p66shc gene protects against age-related endothelial dysfunction. *Circulation* 110, 2889-2895.

Fung, E., and Helisch, A. (2012). Macrophages in collateral arteriogenesis. *Frontiers in physiology* 3, 353.

Galkina, E., Kadi, A., Sanders, J., Varughese, D., Sarembock, I.J., and Ley, K. (2006). Lymphocyte recruitment into the aortic wall before and during development of atherosclerosis is partially L-selectin dependent. *J Exp Med* 203, 1273-1282.

Gautier, E.L., Shay, T., Miller, J., Greter, M., Jakubzick, C., Ivanov, S., Helft, J., Chow, A., Elpek, K.G., Gordonov, S., *et al.* (2012). Gene-expression profiles and transcriptional regulatory pathways that underlie the identity and diversity of mouse tissue macrophages. *Nat Immunol* 13, 1118-1128.

Gerhardt, H., and Betsholtz, C. (2003). Endothelial-pericyte interactions in angiogenesis. *Cell and tissue research* 314, 15-23.

Ginhoux, F., and Jung, S. (2014). Monocytes and macrophages: developmental pathways and tissue homeostasis. *Nat Rev Immunol* 14, 392-404.

Ginhoux, F., Schultze, J.L., Murray, P.J., Ochando, J., and Biswas, S.K. (2015). New insights into the multidimensional concept of macrophage ontogeny, activation and function. *Nat Immunol* 17, 34-40.

Gotschy, A., Bauer, E., Schrod, C., Lykowsky, G., Ye, Y.X., Rommel, E., Jakob, P.M., Bauer, W.R., and Herold, V. (2013). Local arterial stiffening assessed by MRI precedes atherosclerotic plaque formation. *Circ Cardiovasc Imaging* 6, 916-923.

Greenwald, S.E. (2007). Ageing of the conduit arteries. *J Pathol* 211, 157-172.

Hashimoto, D., Chow, A., Noizat, C., Teo, P., Beasley, M.B., Leboeuf, M., Becker, C.D., See, P., Price, J., Lucas, D., *et al.* (2013). Tissue-resident macrophages self-maintain locally throughout adult life with minimal contribution from circulating monocytes. *Immunity* 38, 792-804.

He, H., Mack, J.J., Guc, E., Warren, C.M., Squadrito, M.L., Kilarski, W.W., Baer, C., Freshman, R.D., McDonald, A.I., Ziyad, S., *et al.* (2016). Perivascular Macrophages Limit Permeability. *Arterioscler Thromb Vasc Biol* 36, 2203-2212.

Hume, D.A., and MacDonald, K.P. (2012). Therapeutic applications of macrophage colony-stimulating factor-1 (CSF-1) and antagonists of CSF-1 receptor (CSF-1R) signaling. *Blood* 119, 1810-1820.

Jackson, D.G. (2018). Hyaluronan in the lymphatics: The key role of the hyaluronan receptor LYVE-1 in leucocyte trafficking. *Matrix Biol*, ahead of print Feb 6.

Johnson, L.A., Banerji, S., Lawrence, W., Gileadi, U., Prota, G., Holder, K.A., Roshorn, Y.M., Hanke, T., Cerundolo, V., Gale, N.W., *et al.* (2017). Dendritic cells enter lymph vessels by hyaluronan-mediated docking to the endothelial receptor LYVE-1. *Nat Immunol* 18, 762-770.

Jongstra-Bilen, J., Haidari, M., Zhu, S.N., Chen, M., Guha, D., and Cybulsky, M.I. (2006). Low-grade chronic inflammation in regions of the normal mouse arterial intima predisposed to atherosclerosis. *J Exp Med* 203, 2073-2083.

Kierdorf, K., Prinz, M., Geissmann, F., and Gomez Perdiguero, E. (2015). Development and function of tissue resident macrophages in mice. *Semin Immunol* 27, 369-378.

Kohn, J.C., Lampi, M.C., and Reinhart-King, C.A. (2015). Age-related vascular stiffening: causes and consequences. *Front Genet* 6, 112.

Kothapalli, D., Liu, S.L., Bae, Y.H., Monslow, J., Xu, T., Hawthorne, E.A., Byfield, F.J., Castagnino, P., Rao, S., Rader, D.J., *et al.* (2012). Cardiovascular protection by ApoE and ApoE-HDL linked to suppression of ECM gene expression and arterial stiffening. *Cell reports* 2, 1259-1271.

Kubota, Y., Takubo, K., Shimizu, T., Ohno, H., Kishi, K., Shibuya, M., Saya, H., and Suda, T. (2009). M-CSF inhibition selectively targets pathological angiogenesis and lymphangiogenesis. *J Exp Med* 206, 1089-1102.

Lacolley, P., Thornton, S.N., and Bezie, Y. (2014). Animal Models for Studies of Arterial Stiffness. In *Blood Pressure and Arterial Wall Mechanics in Cardiovascular Diseases*, M.E. Safar, M.F. O'Rourke, and E.D. Frohlich, eds. (London: Springer London), pp. 63-74.

Li, J., Chen, K., Zhu, L., and Pollard, J.W. (2006). Conditional deletion of the colony stimulating factor-1 receptor (c-fms proto-oncogene) in mice. *Genesis* 44, 328-335.

Lim, H.Y., Thiam, C.H., Yeo, K.P., Bissoondial, R., Hii, C.S., McGrath, K.C., Tan, K.W., Heather, A., Alexander, J.S., and Angeli, V. (2013). Lymphatic vessels are essential for the removal of cholesterol from peripheral tissues by SR-BI-mediated transport of HDL. *Cell metabolism* 17, 671-684.

Lopez-De Leon, A., and Rojkind, M. (1985). A simple micromethod for collagen and total protein determination in formalin-fixed paraffin-embedded sections. *J Histochem Cytochem* 33, 737-743.

Majesky, M.W., Dong, X.R., Hogg, V., Mahoney, W.M., Jr., and Daum, G. (2011). The adventitia: a dynamic interface containing resident progenitor cells. *Arterioscler Thromb Vasc Biol* 31, 1530-1539.

Mitchell, G.F., Hwang, S.J., Vasan, R.S., Larson, M.G., Pencina, M.J., Hamburg, N.M., Vita, J.A., Levy, D., and Benjamin, E.J. (2010). Arterial stiffness and cardiovascular events: the Framingham Heart Study. *Circulation* 121, 505-511.

Moore, J.P., Vinh, A., Tuck, K.L., Sakkal, S., Krishnan, S.M., Chan, C.T., Lieu, M., Samuel, C.S., Diep, H., Kemp-Harper, B.K., *et al.* (2015). M2 macrophage accumulation in the aortic wall during angiotensin II infusion in mice is associated with fibrosis, elastin loss, and elevated blood pressure. *Am J Physiol Heart Circ Physiol* 309, H906-917.

Murakami, M., and Simons, M. (2009). Regulation of vascular integrity. *J Mol Med (Berl)* 87, 571-582.

Murata K, M.T., Kotake C (1986). Collagen types in various layers of the human aorta and their changes with the atherosclerotic process. *Atherosclerosis* 60, 251-262.

Murayama, T., Yokode, M., Kataoka, H., Imabayashi, T., Yoshida, H., Sano, H., Nishikawa, S., Nishikawa, S., and Kita, T. (1999). Intraperitoneal administration of anti-c-fms monoclonal antibody prevents initial events of atherogenesis but does not reduce the size of advanced lesions in apolipoprotein E-deficient mice. *Circulation* 99, 1740-1746.

Murphy, G., and Nagase, H. (2011). Localizing matrix metalloproteinase activities in the pericellular environment. *The FEBS journal* 278, 2-15.

Oga, T., Matsuoka, T., Yao, C., Nonomura, K., Kitaoka, S., Sakata, D., Kita, Y., Tanizawa, K., Taguchi, Y., Chin, K., *et al.* (2009). Prostaglandin F(2alpha) receptor signaling facilitates bleomycin-induced pulmonary fibrosis independently of transforming growth factor-beta. *Nat Med* 15, 1426-1430.

Ohno, H., Kubo, K., Murooka, H., Kobayashi, Y., Nishitoba, T., Shibuya, M., Yoneda, T., and Ise, T. (2006). A c-fms tyrosine kinase inhibitor, Ki20227, suppresses osteoclast differentiation and osteolytic bone destruction in a bone metastasis model. *Mol Cancer Ther* 5, 2634-2643.

Owens, G.K., Kumar, M.S., and Wamhoff, B.R. (2004). Molecular regulation of vascular smooth muscle cell differentiation in development and disease. *Physiological reviews* 84, 767-801.

Palombo, C., and Kozakova, M. (2016). Arterial stiffness, atherosclerosis and cardiovascular risk: Pathophysiologic mechanisms and emerging clinical indications. *Vascul Pharmacol* 77, 1-7.

Pham, T.H., Baluk, P., Xu, Y., Grigorova, I., Bankovich, A.J., Pappu, R., Coughlin, S.R., McDonald, D.M., Schwab, S.R., and Cyster, J.G. (2010). Lymphatic endothelial cell sphingosine kinase activity is required for lymphocyte egress and lymphatic patterning. *J Exp Med* 207, 17-27.

Pinto, A.R., Paolicelli, R., Salimova, E., Gospocic, J., Slonimsky, E., Bilbao-Cortes, D., Godwin, J.W., and Rosenthal, N.A. (2012). An abundant tissue macrophage population in the adult murine heart with a distinct alternatively-activated macrophage profile. *PloS one* 7, e36814.

Randolph, G.J. (2014). Mechanisms that regulate macrophage burden in atherosclerosis. *Circ Res* 114, 1757-1771.

Redondo-Munoz, J., Ugarte-Berzal, E., Garcia-Marco, J.A., del Cerro, M.H., Van den Steen, P.E., Opdenakker, G., Terol, M.J., and Garcia-Pardo, A. (2008). Alpha4beta1 integrin and 190-kDa CD44v

constitute a cell surface docking complex for gelatinase B/MMP-9 in chronic leukemic but not in normal B cells. *Blood* 112, 169-178.

Rensen, S.S., Doevendans, P.A., and van Eys, G.J. (2007). Regulation and characteristics of vascular smooth muscle cell phenotypic diversity. *Neth Heart J* 15, 100-108.

Schlereth, S.L., Neuser, B., Caramoy, A., Grajewski, R.S., Koch, K.R., Schrod, F., Cursiefen, C., and Heindl, L.M. (2014). Enrichment of lymphatic vessel endothelial hyaluronan receptor 1 (LYVE1)-positive macrophages around blood vessels in the normal human sclera. *Investigative ophthalmology & visual science* 55, 865-872.

Simons, M., and Eichmann, A. (2015). Molecular controls of arterial morphogenesis. *Circ Res* 116, 1712-1724.

Swirski, F.K., Robbins, C.S., and Nahrendorf, M. (2016). Development and Function of Arterial and Cardiac Macrophages. *Trends Immunol* 37, 32-40.

Tamoutounour, S., Williams, M., Montanana Sanchis, F., Liu, H., Terhorst, D., Malosse, C., Pollet, E., Ardouin, L., Luche, H., Sanchez, C., *et al.* (2013). Origins and functional specialization of macrophages and of conventional and monocyte-derived dendritic cells in mouse skin. *Immunity* 39, 925-938.

Tamoutounour, S., Henri, S., Lelouard, H., de Bovis, B., de Haar, C., van der Woude, C.J., Woltman, A.M., Rey, Y., Bonnet, D., Sichien, D., *et al.* (2012). CD64 distinguishes macrophages from dendritic cells in the gut and reveals the Th1-inducing role of mesenteric lymph node macrophages during colitis. *Eur J Immunol* 42, 3150-3166.

Tan, C.K., Tan, E.H., Luo, B., Huang, C.L., Loo, J.S., Choong, C., and Tan, N.S. (2013). SMAD3 deficiency promotes inflammatory aortic aneurysms in angiotensin II-infused mice via activation of iNOS. *Journal of the American Heart Association* 2, e000269.

Thomas, A.C., and Newby, A.C. (2010). Effect of matrix metalloproteinase-9 knockout on vein graft remodelling in mice. *J Vasc Res* 47, 299-308.

Tsamis, A., Krawiec, J.T., and Vorp, D.A. (2013). Elastin and collagen fibre microstructure of the human aorta in ageing and disease: a review. *Journal of the Royal Society, Interface / the Royal Society* 10, 20121004.

Vafaie, F., Yin, H., O'Neil, C., Nong, Z., Watson, A., Arpino, J.M., Chu, M.W., Wayne Holdsworth, D., Gros, R., and Pickering, J.G. (2014). Collagenase-resistant collagen promotes mouse aging and vascular cell senescence. *Aging cell* 13, 121-130.

Varol, C., Mildner, A., and Jung, S. (2015). Macrophages: development and tissue specialization. *Annu Rev Immunol* 33, 643-675.

Vlachopoulos, C., Aznaouridis, K., and Stefanadis, C. (2010). Prediction of cardiovascular events and all-cause mortality with arterial stiffness: a systematic review and meta-analysis. *Journal of the American College of Cardiology* 55, 1318-1327.

Wagenseil, J.E., and Mecham, R.P. (2009). Vascular extracellular matrix and arterial mechanics. *Physiological reviews* 89, 957-989.

Wagenseil, J.E., Nerurkar, N.L., Knutsen, R.H., Okamoto, R.J., Li, D.Y., and Mecham, R.P. (2005). Effects of elastin haploinsufficiency on the mechanical behavior of mouse arteries. *Am J Physiol Heart Circ Physiol* 289, H1209-1217.

Wang, Y., Ait-Oufella, H., Herbin, O., Bonnin, P., Ramkhelawon, B., Taleb, S., Huang, J., Offenstadt, G., Combadiere, C., Renia, L., *et al.* (2010). TGF-beta activity protects against inflammatory aortic aneurysm progression and complications in angiotensin II-infused mice. *J Clin Invest* 120, 422-432.

Xu, H., Chen, M., Reid, D.M., and Forrester, J.V. (2007). LYVE-1-positive macrophages are present in normal murine eyes. *Investigative ophthalmology & visual science* 48, 2162-2171.

Yabluchanskiy, A., Ma, Y., Iyer, R.P., Hall, M.E., and Lindsey, M.L. (2013). Matrix metalloproteinase-9: Many shades of function in cardiovascular disease. *Physiology (Bethesda)* 28, 391-403.

Yu, Q., and Stamenkovic, I. (2000). Cell surface-localized matrix metalloproteinase-9 proteolytically activates TGF-beta and promotes tumor invasion and angiogenesis. *Genes Dev* 14, 163-176.

Zeisel, A., Munoz-Manchado, A.B., Codeluppi, S., Lonnerberg, P., La Manno, G., Jureus, A., Marques, S., Munguba, H., He, L., Betsholtz, C., *et al.* (2015). Brain structure. Cell types in the mouse cortex and hippocampus revealed by single-cell RNA-seq. *Science* 347, 1138-1142.

Zhang, H., Tse, J., Hu, X., Witte, M., Bernas, M., Kang, J., Tilahun, F., Hong, Y.K., Qiu, M., and Chen, L. (2010). Novel discovery of LYVE-1 expression in the hyaloid vascular system. *Investigative ophthalmology & visual science* 51, 6157-6161.

## Figure Legends

### Figure 1. Depletion of aortic-resident macrophages leads to arterial wall remodeling (A)

Dot plots show gating strategy for aortic macrophages (mean  $\pm$  SEM, n=6). Numbers adjacent to outlined area denotes percentage of macrophage subsets. (B) Aortic sections stained for Col I, SMA (smooth muscle actin) and CD68 (arrows). Asterisk denotes SMA<sup>+</sup> media. (C) Aortic macrophages quantification in adventitia and media/intima by flow cytometry (mean  $\pm$  SEM, n= 2). (D) Normalised gene expression of *Csf1* and *Csf1r* in the intima/media and adventitia of WT aorta (mean  $\pm$  SEM; n = 5 per group). (E) Flow cytometry analysis of CSF-1R expression by aortic macrophages. (F) Aortic sections of MaFIA mice showing CSF-1R expression on adventitial macrophages. Arrows indicate CSF-1R positive macrophages. (G-H) WT mice received daily oral gavage of Ki20227 for 2 weeks. (G) Aortic macrophages number for vehicle- and Ki20227-treated WT mice determined by flow cytometry (mean  $\pm$  SEM; n = 13 per group). (H) CD68<sup>+</sup> macrophages in aortic sections after vehicle or Ki20227 treatment. (I-N) Analysis of descending aortas from WT mice treated with Ki20227 or vehicle for 14 weeks. (I) Aortic macrophages number (mean  $\pm$  SEM; n = 4 per group). (J) Representative image of aortic sections immunostained for CD68 and SMA. Media elastic lamella is auto-fluorescent (green). Inserts show high magnification images. (K) Distance of aortic CD68<sup>+</sup> macrophages from medial external elastin lamella (EEL), (L) average luminal diameter and (M) adventitial area (mean  $\pm$  SEM; n = 7-9 per group). (N) Double immunostaining for Col I and SMA showing expanded adventitial area in Ki20227-

treated WT aortas. All data are collected from 2-3 independent experiments. \* $p < 0.05$ \*\* $p < 0.005$ ; \*\*\* $p < 0.0005$ . Scale bar = 100  $\mu\text{m}$  except B and F = 50  $\mu\text{m}$ .

**Figure 2. Resident macrophages regulate vessel function and ECM content (A-G)**

Analysis of descending aortas from mice treated with Ki20227 or vehicle for 14 weeks. Relative gene expression in media and intima (A), and adventitia (B) with  $n = 5-10$  per group (mean  $\pm$  SEM). (C) Quantification of aorta collagen content using Sirius red (mean  $\pm$  SEM,  $n = 6-7$ ). (D) Sirius Red stained aortic sections showed increased collagen content in adventitia and media of Ki20227-treated groups. (E-G) Biomechanical properties of aortas from Ki20227-treated and vehicle-treated mice in circumferential tensile and contractility tests. (E) Stress-strain curve, (F) stiffness and (G) maximal contractile force in response to KCI stimulus (mean  $\pm$  SEM with  $n = 5-7$  mice). (H-P) WT mice received daily oral gavage of vehicle or Ki20227 for 24 weeks. Recovery WT mice group received Ki20227 for the first 14 weeks to induce arterial remodelling and, then switched to vehicle for another 10 weeks. (H) Aortic macrophages number for vehicle-, Ki20227- and recovery-treated WT mice determined by flow cytometry (mean  $\pm$  SEM;  $n = 7-8$  per group). (I) Representative image of aortic sections immunostained for CD68 and SMA. Inserts show high magnification images. (J) Engraftment of aortic CD45.1<sup>+</sup> BM cells in irradiated CD45.2 recipients assessed by flow cytometry 8 weeks after treatment with Ki20227 or vehicle (mean  $\pm$  SEM;  $n = 3-4$  per group) (K) Double immunostaining for Col I and SMA delineated adventitial and medial layer. (L) Average luminal diameter and (M) adventitial area (mean  $\pm$  SEM;  $n = 5-6$  per group). (N) Quantification of aorta collagen content using Sirius red (mean  $\pm$  SEM,  $n = 6-7$  per group). (O and P) Mechanical testing of the descending thoracic aorta. (O) Aortic stiffness and (P) maximal contractile force in response to KCI stimulus (mean  $\pm$  SEM,  $n = 6-11$  per group). (Q-Y) High fat diet fed *ApoE*<sup>-/-</sup> mice at 9-10 weeks of age received daily oral administration of Ki20227 or vehicle for 9 weeks. Descending aorta sections stained for CD68 in (Q) and

Col I in (S) with SMA and DAPI co-stain. (R) Average luminal diameter and (T) adventitial area (mean  $\pm$  SEM; n = 4-7 per group). (U) Aortic stiffness and (V) maximal contractile force in response to KCl stimulus (mean  $\pm$  SEM, n = 8-10 per group). (W) Systolic, (X) diastolic and (Y) mean blood pressure (mean  $\pm$  SEM, n = 5-6 per group). Data are pooled from 2-3 independent experiments. \*p < 0.05; \*\*P < 0.005; \*\*\*P < 0.0005. Scale bar = 100  $\mu$ m.

**Figure 3. Phenotype of aortic macrophages** (A) Aorta whole mount stained for LYVE-1. (B) Dot plots show gating strategy for aortic macrophages (mean  $\pm$  SEM, n=6). Numbers adjacent to outlined area denotes percentage of macrophage subsets. (C) Aortic sections stained for Col I, SMA and LYVE-1 (arrows). Asterisk denotes SMA<sup>+</sup> media. (D) Aortic sections stained for LYVE-1, CD68 and SMA. (E) Aortic sections stained for LYVE-1, MHC-II and CD31. Pink arrows and yellow arrows indicate LYVE-1<sup>+</sup>MHCII<sup>-</sup> and LYVE-1<sup>+</sup>MHCII<sup>+</sup> macrophages, respectively. (F) LYVE-1<sup>+</sup>MHC-II<sup>-</sup>, LYVE-1<sup>+</sup>MHC-II<sup>+</sup> and LYVE-1<sup>-</sup>MHC-II<sup>+</sup> macrophage quantification in adventitia and media/intima by flow cytometry (mean  $\pm$  SEM, n= 2). (G) Aortic sections of MaFIA mice showing CSF-1R expression on LYVE-1<sup>+</sup> macrophages. (H) Flow cytometry analysis of CSF-1R expression by LYVE-1<sup>+</sup>MHC-II<sup>-</sup>, LYVE-1<sup>+</sup>MHC-II<sup>+</sup> and LYVE-1<sup>-</sup>MHC-II<sup>+</sup> aortic macrophages. (I and J) WT mice received daily oral gavage of Ki20227 for 2 weeks. (I) Aortic macrophages number for vehicle- and Ki20227-treated WT mice determined by flow cytometry (mean  $\pm$  SEM; n = 13 per group). (J) LYVE-1<sup>+</sup> macrophages in aortic sections after vehicle or Ki20227 treatment. All data are collected from 2-3 independent experiments. \*\*\*p < 0.0005. Scale bar = 50  $\mu$ m except J = 100  $\mu$ m.



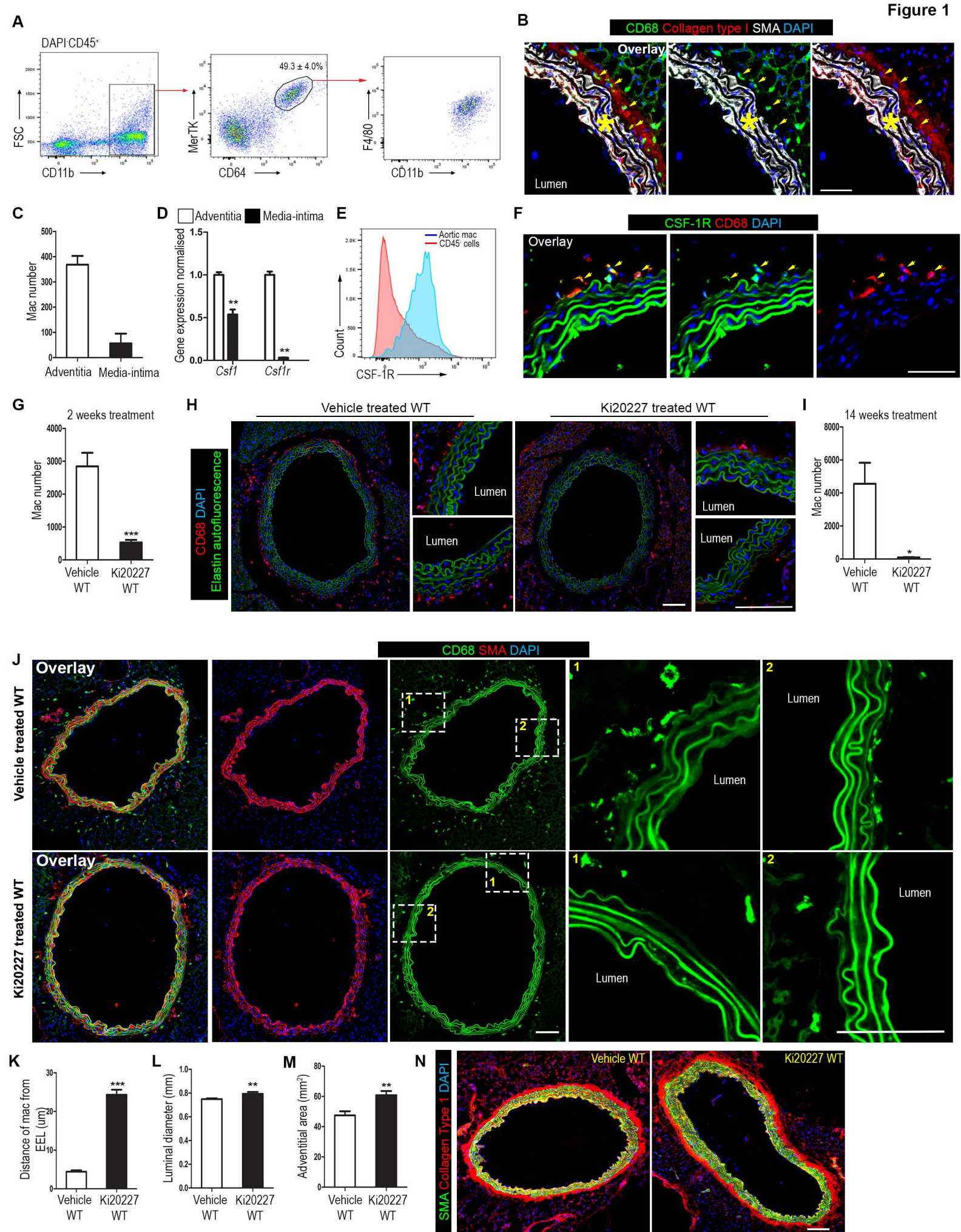
**Figure 4. LYVE-1<sup>+</sup> macrophages are associated with vascular SMCs** (A) Extended views of ear whole mounts for LYVE-1, CD31 and collagen (second harmonic generation), starting from the dermoepidermal junction. White arrows and arrowheads indicate non-perivascular and perivascular LYVE-1<sup>+</sup> macrophages respectively. (B and C) Confocal images of ear whole mount stained for LYVE-1, SMA (B) and CD31 (C). Dotted white lines illustrate the train track patterning by LYVE-1<sup>+</sup> cells. Yellow arrowheads indicate perivascular LYVE-1<sup>+</sup> macrophages while yellow arrows denote initial lymphatics in (B) and capillaries in (C). (D) LYVE-1<sup>+</sup> cells lining SMA<sup>+</sup> blood vessels in ear whole mount were CD68<sup>+</sup>CD206<sup>+</sup>MHC-II<sup>+</sup>. LYVE-1<sup>+</sup> macrophages are associated with pial, pial penetrating (E) and parenchymal (F) SMC<sup>+</sup> vessels of the brain. (G) Adipose tissue sections stained for LYVE-1, CD68, SMA and DAPI. Yellow arrows indicate perivascular macrophages (H) Human skin stained for LYVE-1, SMA and CD31. (I) Human umbilical cord sections stained for LYVE-1 and SMA identified LYVE-1<sup>+</sup> cells surrounding SMA<sup>+</sup> arteries and vein. Images are representative of at least 3-10 mice/human samples for each condition examined. Scale bar = 50  $\mu$ m except E, F, H and I = 100  $\mu$ m.

**Figure 5. Specific depletion of aortic-resident LYVE-1<sup>+</sup> macrophages leads to arterial wall remodelling and dysfunction** (A-C) LYVE-1<sup>+</sup> and LYVE-1<sup>-</sup> macrophages from aorta were sorted (3 replicates), RNA was extracted and transcriptomic profiling was performed. (A) Heat map showing differential expressed genes between aortic LYVE-1<sup>+</sup> and LYVE-1<sup>-</sup> macrophages. (B and C) Histogram of aortic LYVE-1<sup>+</sup> and LYVE-1<sup>-</sup> macrophages with specific gene functions based on GO classification. (D-S) Aortas from 16 weeks old *Lyve-1<sup>wt/Cre</sup>;Csflr<sup>flox/flox</sup>* and *Csflr<sup>flox/flox</sup>* mice were obtained for analysis. (D-H) Macrophages and monocytes number for *Lyve-1<sup>wt/Cre</sup>;Csflr<sup>flox/flox</sup>* and *Csflr<sup>flox/flox</sup>* mice determined by flow cytometry (mean  $\pm$  SEM; n = 6-8 per group). (I) Representative image of aortic sections immunostained for LYVE-1 and CD68. Media elastic lamella is auto-fluorescent (green).

Inserts show high magnification images. (J) Double immunostaining for Col I and SMA showing expanded adventitial area in *Lyve-1<sup>wt/Cre</sup>;Csf1r<sup>flx/flx</sup>* aortas compared to *Csf1r<sup>flx/flx</sup>* aortas. (K) Average luminal diameter and (L) adventitial area (mean  $\pm$  SEM; n = 5 per group). (M) Sirius Red stained aortic sections indicated increased collagen content in adventitia and media of *Lyve-1<sup>wt/Cre</sup>;Csf1r<sup>flx/flx</sup>* groups. (N) Quantification of aorta collagen content using Sirius red (mean  $\pm$  SEM, n = 7). Biomechanical properties of aortas using circumferential tensile and contractility tests. (O) Stiffness and (P) maximal contractile force in response to KCI stimulus (mean  $\pm$  SEM with n = 6-11 mice). (Q) Systolic, (R) diastolic and (S) mean blood pressure (mean  $\pm$  SEM, n = 5-7 per group). All data are collected from 2-3 independent experiments. \*p < 0.05; \*\*p < 0.005; \*\*\*p < 0.0005. Scale bar = 100  $\mu$ m.

**Figure 6. LYVE-1<sup>+</sup> macrophages regulation of collagen expression by SMCs relies on MMP-9 and engagement of HA-LYVE-1 interaction** (A-B) Primary mouse aortic SMCs co-cultured with LYVE-1<sup>+</sup> macrophages, or LYVE-1<sup>-</sup> macrophages for 24h and stained for collagen type I (mean  $\pm$  SEM, n = 5-9 per group). (C) RT-PCR analysis of *Mmp-9* on sorted LYVE-1<sup>+</sup> and LYVE-1<sup>-</sup> macrophages (D) Immunofluorescence for MMP-9, LYVE-1, SMA and DAPI in WT aortic sections. (E) Representative images of gelatin *in situ* zymography in aorta sections. Asterisks denote the medial layer. Pink arrows and yellow arrows indicate fluorescence signal from periaortic layer and adventitial layer, respectively. (F-G) MMP-9 inhibitor was added to SMCs 2h prior to add LYVE-1<sup>+</sup> macrophages for 24h (mean  $\pm$  SEM, n = 2-5 per group). (H-I) SMCs co-cultured with MMP-9<sup>-/-</sup> and MMP-9<sup>+/+</sup> LYVE-1<sup>+</sup> macrophages for 24h (mean  $\pm$  SEM, n = 3-4 per group). (J) SMCs co-cultured with LYVE-1<sup>+</sup> macrophages via direct contact or separated by transwell membrane (n = 2 per group). (K) LYVE-1<sup>+</sup> macrophages were pre-incubated with rat IgG, or anti-LYVE-1 mAb mAb2125, or C1/8 for 30 minutes prior to add to SMCs for 24h (mean  $\pm$  SEM, n = 2-3 per group). (L) SMCs were pre-treated with or without hyaluronidase (Hase) for 2h and co-cultured with

LYVE-1<sup>+</sup> macrophages in the presence of vehicle or 4-MU for 24h (mean  $\pm$  SEM, n = 3-6 per group). Col I expression was measured by outlining the SMCs with smooth muscle actin staining and normalized to non-treated group. Data are pooled from two independent experiments. \*p < 0.05; \*\*p < 0.005; \*\*\*p < 0.0005. Scale bar = 100  $\mu$ m except D and E = 50  $\mu$ m.





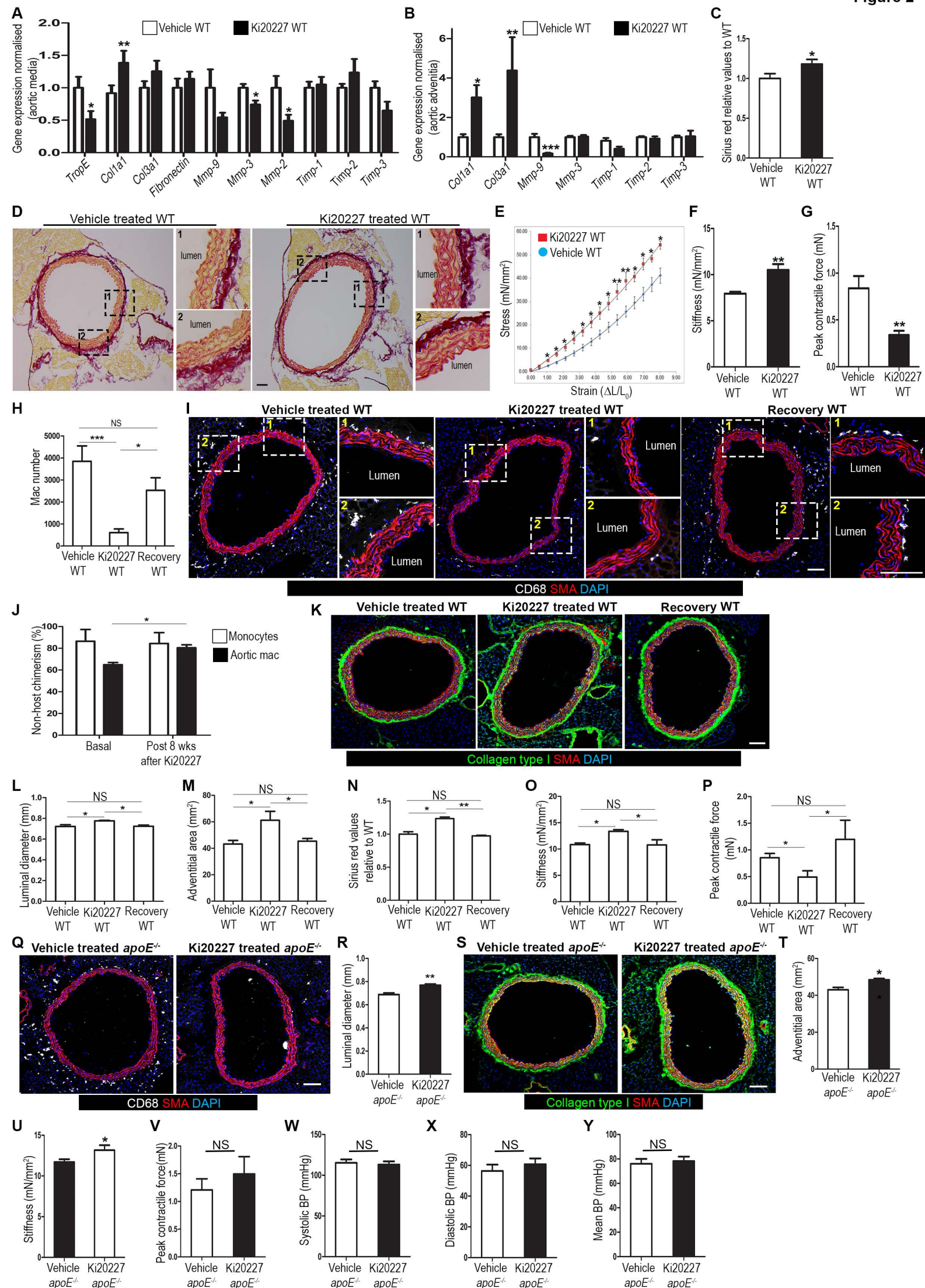




Figure 3

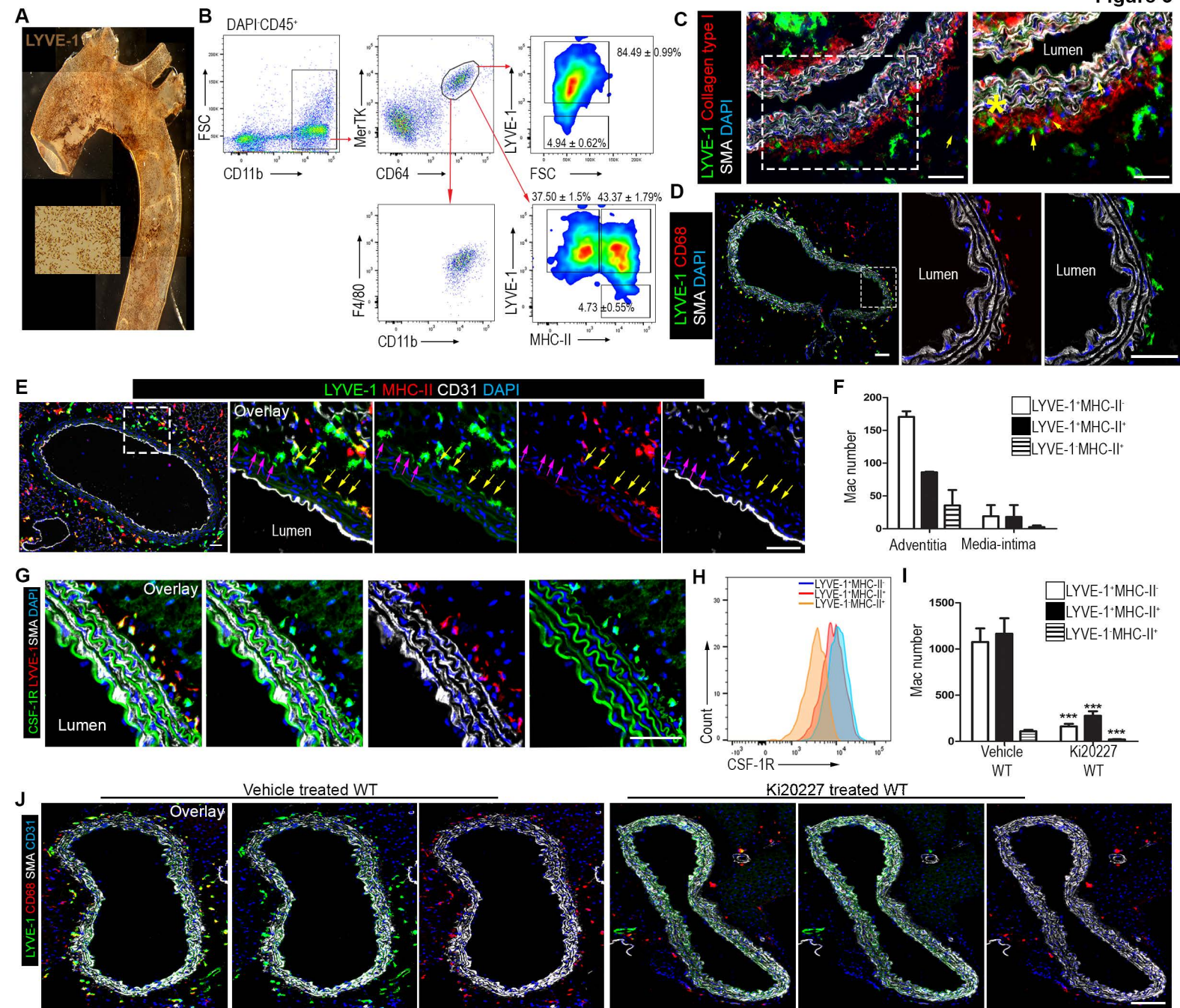




Figure 4

